

Corina SOSDEAN¹, Liviu MARSAVINA², Geert De SCHUTTER³**EXPERIMENTAL AND NUMERICAL INVESTIGATIONS OF THE INFLUENCE OF REAL
CRACKS ON CHLORIDE INGRESS IN CONCRETE****Abstract**

Experimental and numerical results of a chloride ingress study conducted on samples drilled from different locations of a reinforced concrete slab, previously loaded until failure, are presented. The experimental part was carried on following the NT Build 492 standard for the non-steady state migration test, then a 3D model was developed using the Abaqus/Standard software based on the FEM in order to simulate chloride ingress in both uncracked and cracked concrete.

Keywords

Experimental program, numerical simulation, real cracks, chloride ingress.

1 INTRODUCTION

The most widely used construction material in the world is reinforced concrete (RC). In the last decades a huge amount of money has been spent on repair or reconstruction of RC structures. As a consequence, a great interest in studying the durability issue of concrete has been shown.

It is known that in real life, most reinforced concrete structures are cracked (e.g. due to extreme loading, aggressive environment or poor workmanship during execution...) and also that chloride ingress and carbonation are the main causes of steel corrosion. Still, the influence of cracks on chloride penetration in RC structures is still not sufficient understood.

When studying the influence of cracks on chloride penetration most researchers focus either on the experimental aspect of this issue either on developing a numerical model that can accurately simulate chloride ingress into concrete.

Numerous experimental programs were developed in order to create cracks in sound concrete. Based on the crack preparation method found in literature, experimental studies can be roughly divided into two groups: destructive and non-destructive methods. Different destructive mechanical loading techniques are used in order to prepare cracks: wedge splitting test [1] three or four-point bending test [2] Brazillian splitting test [3] and expansive core method [4]. Non-destructive methods used to generate cracks in concrete include studies based on the positioning and removal of thin copper sheets before final setting of concrete [5], or inducing a crack by saw-cutting concrete cylinders longitudinally [6].

¹ Dr.-Ing. Corina Sosdean, Politehnica University of Timisoara, Department Strength of Materials, Blvd. M. Viteazu, No. 1, Timisoara 300222, Romania, phone: +0256403631 email: corina.sosdean@yahoo.com

² Dr.-Ing. Liviu Marsavina, Politehnica University of Timisoara, Department Strength of Materials, Blvd. M. Viteazu, no. 1, Timisoara 300222, Romania, phone: +40256403577 email: msvina@mec.upt.ro Timisoara 300222, Romania, phone: +40256403577 email: msvina@mec.upt.ro

³ Dr.-Ing. Geert De Schutter, Ghent University, Magel Laboratory for Concrete Research, Department of Structural Engineering Technologiepark-Zwijnaarde 904, B-9052 Ghent, Belgium, phone: +3292645521 email: Geert.DeSchutter@UGent.be

Also, various numerical and modeling techniques were developed for analyzing the two or three- dimensional aspects of chloride ingress in cracked concrete by taking into account its different transport mechanisms. In most of the cases, the transport of chloride ions into concrete is considered as pure diffusion and it's solved as a one-dimensional in a semi-infinite medium according to Fick's 2nd law of diffusion and most numerical models adopt the geometrical patterns of the cracks in accordance with the samples used in the experiments. Based on the different existing procedures, they were classified by [7] in: rectangular crack, cracking wall acts as exposed surface [5],[8], rectangular cracks, width-dependent chloride diffusion coefficient in crack [9], realistic crack, width-dependent chloride diffusion coefficient in crack [10], load induced crack, width-dependant chloride diffusion coefficient in crack [11]. Some researchers considered not only diffusion as a transport mechanism, but also migration, convection/capillary suction, permeation, and chloride binding [12].

Due to the fact that real cracks in concrete have a complex 3D geometry and their influence on transport and degradation mechanisms is not straightforward, very limited investigation of the influence of chloride diffusion on samples with real cracks has been conducted.

In present work the influence of real cracks in reinforced concrete structures subjected to chloride ingress is studied, by presenting both the experimental program and a numerical model that can accurately simulate chloride penetration in uncracked and cracked concrete samples.

2 EXPERIMENTAL PROGRAM

2.1 Sample preparation

40 cores of 100 mm diameter and 50 mm thickness were drilled from various locations of RC slab (Figure 1) exposed to an artificial failure of the central support and subsequent vertical loading until collapse. A detailed description of the test set-up of the slab and the results for the experimental large-scale tests are described in [13].

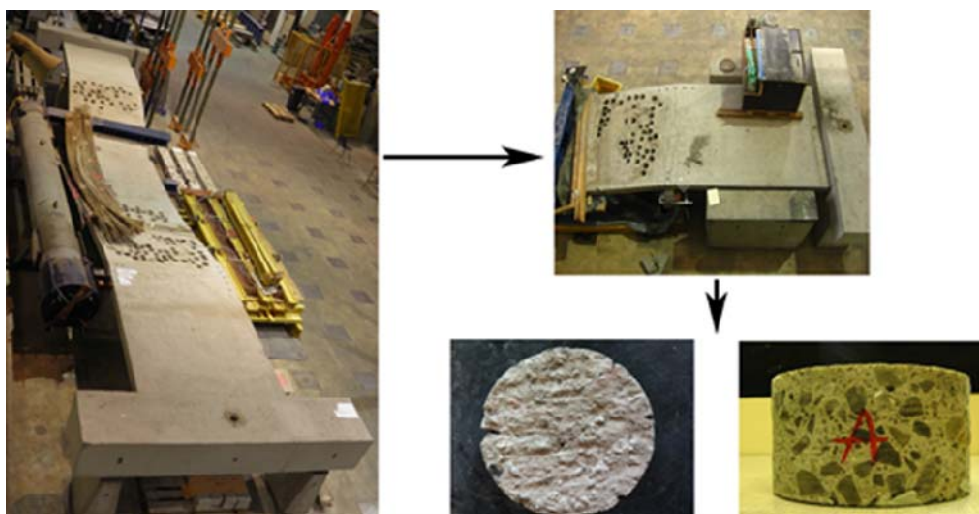


Fig. 1. Slab after the drilling of the cores [16]

The obtained samples can be categorized in four main groups: samples without cracks and without rebars (S) (a), samples with cracks and without rebars (SC) (b), samples without cracks and with rebars (SR) (c), samples with cracks and with rebars (SCR) (d), as it can be observed in Figure 2, where a representative sample for each group is presented.

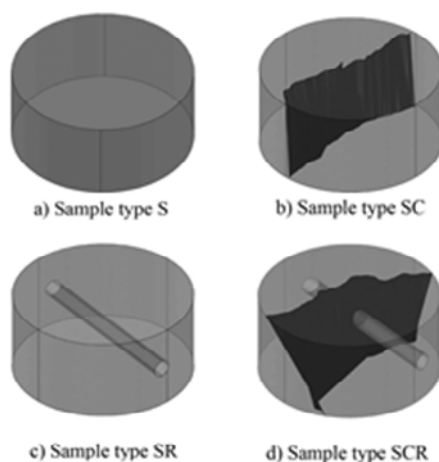


Fig. 2. Sample categories [14]

2.2 Experimental test set-up and test procedure

Chloride ingress was simulated in the concrete samples by performing a non-steady state migration test, according to [15]. Prior testing, the samples were placed in a vacuum container for vacuum treatment for three hours to a pressure in the range of 10-50 mbar; afterwards with the vacuum pump still running, the container was filled with saturated $\text{Ca}(\text{OH})_2$ solution so as to immerse all specimens which was maintained for a further hour before allowing air to re-enter the container. The specimens were kept in the solution for 18 ± 2 hours. A schematic representation of this procedure can be observed in Figure 3.

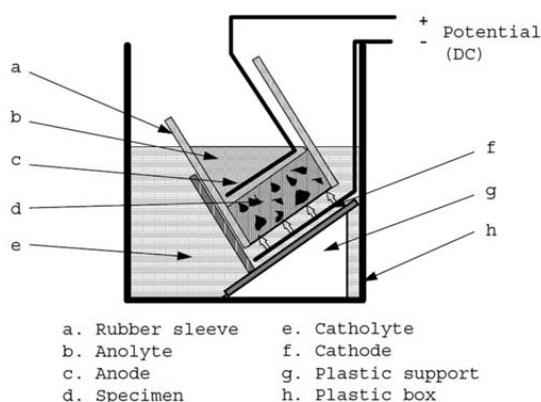


Fig. 3. Test setup of non-steady state migration test (according to [15])

The samples were then placed in the reservoir and an external electrical potential of 30 and 35V was applied for 24 h, forcing the chloride ions from the 10% NaCl solution to migrate into the specimens.

2.3 Penetration depth

The chloride penetration profile was determined by using the colorimetric method [16]. First, all samples were split perpendicular to the crack path: samples type S were split in two, while samples type SR, SC and SCR were cut in 6 parts each; then, all cut parts were sprayed with 0.01N AgNO_3 solution and the mean chloride penetration profiles were determined (Figure 5).

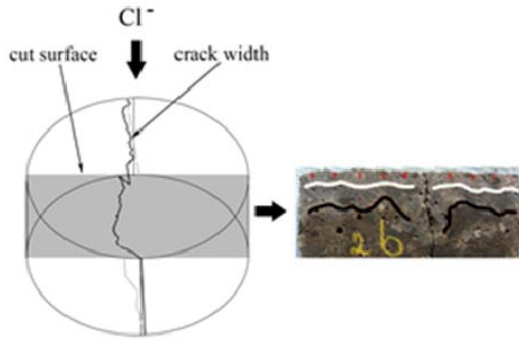


Fig. 5. Sample preparation for measuring the chloride front [14]

The average chloride depth (x_d) and the chloride depth near the crack (x_c) were determined. A more detailed description about this procedure can be found in [14]. A schematic representation of the chloride depths measurement in the middle of the sample is presented in Figure 6.

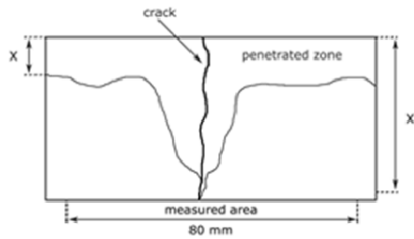


Figure 6. Chloride front measurement in the middle of the sample [16]

Based on the chloride penetration depth the chloride migration coefficient (D_{nssm}) can be calculated according to Equation 1:

$$D_{nssm} = \frac{RT}{z \cdot FE} \cdot \frac{x_d - \alpha \sqrt{x_d}}{t}, \quad (1)$$

where

$$E = \frac{U - 2}{L}$$

$$\alpha = 2 \sqrt{\frac{RT}{zFE} \cdot \operatorname{erf}^{-1} \left(1 - \frac{2c_d}{c_0} \right)} \quad (2)$$

c_d chloride concentration at which the color changes ($= 0.07N$),

c_0 chloride concentration in the catholyte solution ($= 2N$),

erf^{-1} inverse of error function,

F Faraday constant ($= 9.648 \times 10^4 \text{ J/(V} \cdot \text{Mol)}$),

L thickness of the specimens (m),

R gas constant ($= 8.314 \text{ J/(K} \cdot \text{Mol)}$),

x_d chloride penetration depth (m),

t test duration (sec),

T average value of the initial and final temperatures in the anolyte solution (K),

U applied voltage (V),

z absolute value of ionic valence ($= 1$ for chloride).

2.4 Experimental results

Based on the relations presented above the migration coefficients corresponding to the average chloride depth (Dd) and the chloride depth near the crack (Dc) were determined for each type of sample. Table 1 corresponds to the migration coefficients for reference samples and Table 2 corresponds to the migration coefficient for samples type SC, SCR, SR.

Tab. 1 Migration coefficient for reference samples type S

Migration coefficient							
$D_d (\times 10^{-12} \text{ m}^2/\text{s})$							
Sample				Sample		Sample	
Ref I a	4.9	Ref I b	7.2	Ref IV a	8.6	Ref IV b	5.4
Ref II a	7	Ref II b	4.6	Ref V	9.8	Ref VII	6.1
Ref III a	8.3	Ref III b	3.4	Ref VI	10.7	Ref VIII	6.5

Tab. 2 Migration coefficient for reference samples type SR, SCR, SC

Migration coefficient ($\times 10^{-12} \text{ m}^2/\text{s}$)								
	D _d	D					D _d	D
Sample			Sample			Sample		
Sample 1R	4.6	3.7	K	11.4	10.1	13	12	9.8
Sample 2R	4.5	4.2	L	9	8.9	16	9.5	9.2
Sample 3R	4.3	3.6	M	11.2	11.6	25	9.7	10.3
Sample 4R	7	5.4	N	9.3	8.7	A2	10.9	12
Sample 6R	8.7	4.9	4	8.8	9.6	B2	10	10.4
Sample 7R	9.5	10	6	5.9	6.6			
J	9.3	8.3	7	11.3	9.3			

2.5 Measurement of crack width

In order to determine the crack width corresponding to each sample, the following procedure was used: cracks were made more visible by applying barium sulphate powder (BaSO_4) - initially the samples were highlighted with a black marker where the cracks were located and then by applying the powder, this filled the cracks and due to the colour contrast cracks became more visible; then, using the optical microscope the crack width was measured in 5 different locations positioned at 2 cm distance from each other, both on the top and bottom surfaces. This procedure is illustrated in Figure 7.

Surface measured average crack widths range from 104 to 372 μm for the top and bottom surfaces of the samples and from 63 to 311 μm for through- thickness of the sample. Table 3 presents the average values of the crack widths determined as a sum of the measurements determined at the top and bottom surface, while Table 4 presents the average values of the crack widths determined through-thickness of the samples.

A more detailed description of the experimental part presented in this research can be found in [16].

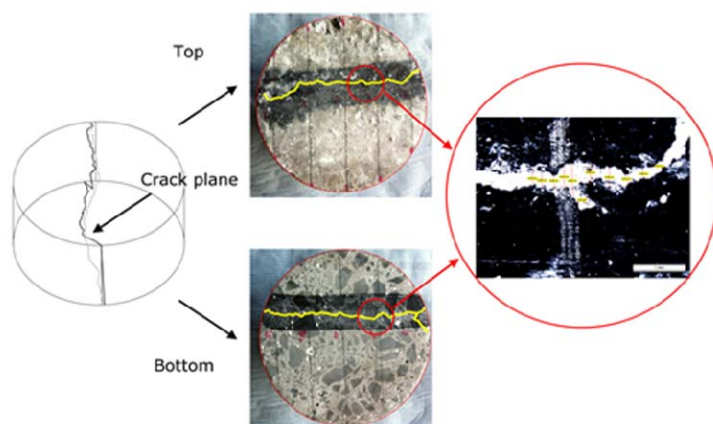


Fig. 7. Measurement of the crack width determination procedure [16]

Tab. 3 Rounded values of crack widths for top/bottom surfaces

Sample	Crack opening (mm)	Sample	Crack opening (mm)
A	0.3	L	0.3
B	0.3	M	0.3
C	0.2	N	0.3
D	0.2	4	0.1
E	0.3	6	0.2
F	0.2	7	0.1
G	0.4	13	0.1
H	0.3	16	0.1
I	0.2	25	0.1
J	0.3	A2	0.2
K	0.3	B2	0.1

Tab. 4 Rounded values of crack widths for through-thickness of the sample

Sample	Crack opening (mm)	Sample	Crack opening (mm)
A	0.2	L	0.1
B	0.2	M	0.2
C	0.1	N	0.1
D	0.1	4	0.2
E	0.3	6	0.3
F	0.2	7	0.1
G	0.1	13	0.1
H	0.1	16	0.2
I	0.2	25	0.1
J	0.1	A2	0.2
K	0.1	B2	0.2

3 NUMERICAL SIMULATION

3.1 Overview of numerical simulation

When simulating chloride transport in cracked concrete, three steps must be taken into consideration: creating the geometry of the crack, determining the chloride transport behavior and determining the numerical method to simulate chloride ingress.

The geometry of the model considered in the numerical simulation was realized taking into consideration the geometrical characteristics of the samples used in the experimental part: cylinders of 100 mm diameter and 50 mm thickness were used in the numerical model. Also, parameters such as: the diffusion coefficient D , initial chloride concentration c and applied chloride concentration C , determined from the experimental part were used as simulation parameters.

3.2 Simulation of chloride penetration in uncracked concrete

Three models having the geometric characteristics previously described in Section 3.1 were considered in order to simulate chloride penetration in sound concrete, in accordance with the reference samples used in the experimental part. 3D 20- node quadratic elements of $2\text{ mm} \times 2\text{ mm} \times 2\text{ mm}$ were used to create the mesh. In order to simulate chloride ingress in accordance with the experimental procedure, the following boundary conditions were considered: on the top surface, a total chloride concentration of 22.045 kg/m^3 corresponding to the 10% NaCl solution was applied, while the other surfaces were considered insulated (0 flux), this being the default condition in Abaqus for mass diffusion. As earlier mentioned in Section 3.1, the diffusion parameters used as simulation parameters were determined experimentally. The diffusivity constants were previously presented in Table 1. In order to determine the value of the initial chloride concentration of 0.03%, corresponding to $c_i = 0.7955\text{ kg/m}^3$, titration was used following the method of [17], then an exponential interpolation was applied to determine the concentration corresponding to the same concentration that was obtained using the silver nitrate solution (1.70 kg/m^3). Figure 8 presents the chloride concentration distribution and the applied boundary conditions.

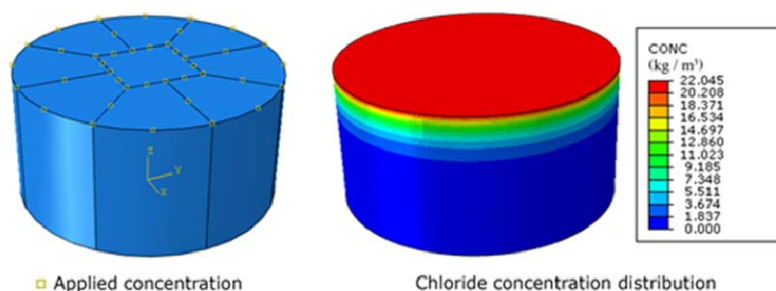


Fig. 8. Applied boundary conditions and chloride concentration distribution [14]

Comparisons between experimental and numerical results on chloride penetration were made and the numerical results were found to be in good agreement with the experimental ones (Figure 9).

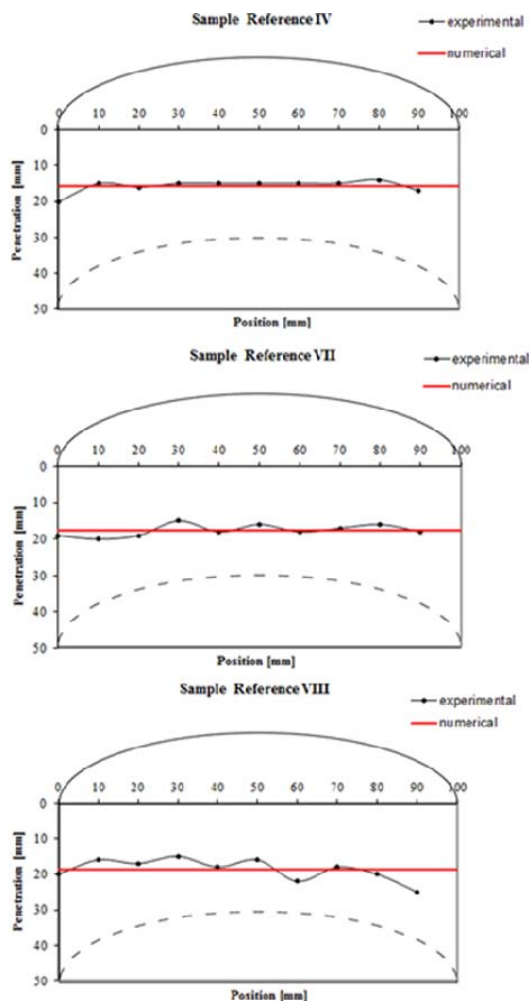


Fig. 9. Comparison between experimental and numerical results for reference samples type S [14]

3.3 Simulation of chloride penetration in cracked concrete

For simulating chloride ingress in cracked concrete, the geometric characteristics of sample type SR: Sample 4 was considered. The same numerical simulation procedure previously described in Section 3.2 was followed, with the difference that the geometry consists in a disc, which is actually half the cylinder of 100 mm diameter and 50 mm thickness previously presented. This simplification was made because it can be observed that the crack passes right through the middle of the sample. Also, in accordance with the experimental part, the disc was divided into 6 parts. The chloride concentration was applied both on the top and the left surface, considered to be the crack edge, due to the fact that in the present study it was concluded that the considered transecting cracks behave like a free concrete surface exposed to chloride ingress. The same conclusion was found in the study of [18]. The value of the diffusivity constant is $D = 6.1 \times 10^{-12} \text{ m}^2/\text{s}$, the medium value of the three diffusion coefficient values, determined in the non-steady state migration test on reference samples type S. The simulation time was calculated with equation (3), based on the diffusion coefficient and the mean penetration experimentally obtained as in the studies of [5].

$$C = C_0 \left[1 - \operatorname{erf} \left(\frac{x}{2\sqrt{Dt}} \right) \right] \quad (3)$$

Figure 11 presents the chloride concentration distribution.

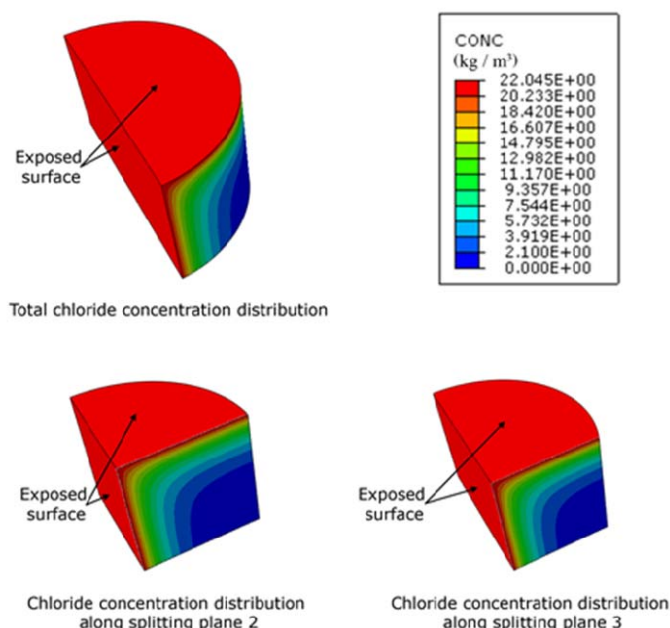


Fig. 11. Chloride concentration distribution [14]

Comparisons between experimental and numerical results on chloride penetration are further presented in Figure 12.

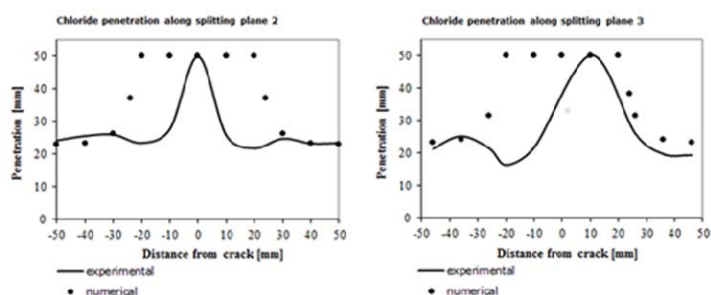


Fig. 12. Comparison between experimental and numerical results [14]

4 CONCLUSIONS

As a conclusion, based on the numerical results which agree fairly well with the experimental ones, it can be said that the proposed numerical model seems to be a good tool to simulate chloride ingress in uncracked and cracked concrete.

ACKNOWLEDGMENT

This work was done in the framework of Bilateral Scientific Agreement between Ghent University, Belgium and Politehnica University of Timisoara, Romania. Also, the financial support of the Special Research Fund (BOF) of Ghent University is gratefully acknowledged.

LITERATURE

- [1] Schlangen, E. et al. *Measurement of chloride ingress in cracked concrete*. In: Audenaert K., Marsavina L., De Schutter G. (eds), International RILEM workshop on transport mechanisms in cracked concrete. Acco, Leuven pp 19-25, 2007, ISBN 978-90-334-6637-3

- [2] Ye, H. et al. Influence of cracking on chloride diffusivity and moisture influential depth in concrete subjected to simulated environmental conditions. *Construction and Building Materials*, 2013, vol. 47, pp. 66-79 ISSN 0950-0618, DOI:10.1016/j.conbuildmat.2013.04.024
- [3] Aldea, C.M. and Shah, S.P. (1999). Effect of cracking on water and chloride permeability of concrete. *Journal of Materials in Civil Engineering*, ASCE, vol. 11(3), pp. 181-187 ISSN (print) 0899-1561, ISSN (online) 1943-5533 DOI:10.1061/(ASCE)0899-1561(1999)11:3(181)
- [4] Ismail, M. et al. Effect of crack opening on the local diffusion of chloride in inert materials. *Cement and Concrete Research*, 2004, vol. 34(4), pp. 711-716 ISSN 0008-8846, DOI:10.1016/j.cemconres.2003.10.025
- [5] Marsavina, L. et al. Experimental and numerical determination of the chloride penetration in cracked concrete. *Construction and Building Materials*, 2009, vol. 23(1), pp. 264-274 ISSN 0950-0618, DOI: 10.1080/19648189.2015.1035802
- [6] Pour-Ghaz, M. et al. Numerical and experimental assessment of unsaturated fluid transport in saw-cut (Notched) concrete elements. *ACI Special Publication SP266-06*, 2009, vol. 266, pp. 73-86
- [7] Gu, C. P., Ye, G., & Sun, W. A review of the chloride transport properties of cracked concrete: experiments and simulations. *Journal of Zhejiang University SCIENCE A*, 2015 16(2), 81-92. ISSN (online)1862-1775, ISSN (print) 1673-565, DOI: 10.1631/jzus.A1400247
- [8] De Schutter, G. Quantification of the influence of cracks in concrete structures on carbonation and chloride penetration. *Magazine of Concrete Research*, 1999a, 51(6), 427-435. ISSN 0024-9831, DOI: 10.1680/mac.1999.51.6.427
- [9] Djerbi, A., Bonnet, S., Khelidj, A. and Baroghel-bouny, V. Influence of traversing crack on chloride diffusion into concrete. *Cement and Concrete Research*, 2008, vol. 38(6), pp. 877-883 ISSN 0008-8846, DOI: 10.1016/j.cemconres.2007.10.007
- [10] Lu, Y., Garboczi, E., Bentz, D., & Davis, J. Modeling of Chloride Transport in Cracked Concrete: A 3-D Image-based Microstructure Simulation. In *Proceedings of the 2012 COMSOL Conference*, 2012, ISBN 9780983968825 0983968829
- [11] Šavija, B., Pacheco, J., & Schlangen, E. Lattice modeling of chloride diffusion in sound and cracked concrete. *Cement and Concrete Composites*, 2013 42, 30-40. ISSN 0958-9465, DOI: 10.1016/j.cemconcomp.2013.05.003
- [12] Ožbolt, J, Balabanic, G, Periškić and Kušter, M. Modelling the effect of damage on transport processes in concrete. *Construction and Building Materials*, 2010, vol 24(9), pp. 1638-1648 . ISSN 0950-0618, DOI: 10.1016/j.conbuildmat.2010.02.028
- [13] Gouverneur, D. et al. Experimental investigation of the load-displacement behavior under catenary action in a restrained reinforced concrete slab strip. *Engineering Structures*, 2013 vol. 49, pp.1007-1016. ISSN 0141-0296, DOI: 10.1016/j.engstruct.2012.12.045
- [14] Sosdean, C. *Experimental and numerical investigations of the influence of cracks on mass diffusion in mortar and concrete* (PhD thesis), Politehnica University of Timisoara, Timisoara, Romania. 2015
- [15] NT BUILD 492. *Concrete, Mortar and Cement-Based Repair Materials: Chloride Migration Coefficient from Non-steady-state Migration Experiments*. NORDTEST, 1999.
- [16] Otsuki, N. et al. Evaluation of AgNO₃ solution spray method for measurement of chloride penetration into hardened cementations matrix materials. *ACI Materials Journal*, 1992, 89 (6), pp. 587-592. ISSN 0889-325X, Doi. 10.1016/0950-0618(93)90002-T
- [17] Yuan, Q. *Fundamental Studies on Test Methods for the Transport of Chloride Ions in Cementitious Materials* (PhD thesis). 2009
- [18] Rodriguez,O.G. *Influence of cracks on chloride ingress into concrete*. (PhD thesis), University of Toronto, Toronto, Canada 2001